



HAL
open science

Unravelling Platinum-Zirconia Interfacial Sites Using CO Adsorption

Frederic C Meunier, Raphael Kdhir, Natalia Potrzebowska, N. Perret, Michèle
Besson

► **To cite this version:**

Frederic C Meunier, Raphael Kdhir, Natalia Potrzebowska, N. Perret, Michèle Besson. Unravelling Platinum-Zirconia Interfacial Sites Using CO Adsorption. *Inorganic Chemistry*, 2019, 58 (12), pp.8021-8029. 10.1021/acs.inorgchem.9b00774 . hal-02174237

HAL Id: hal-02174237

<https://hal.science/hal-02174237>

Submitted on 11 Aug 2021

HAL is a multi-disciplinary open access archive for the deposit and dissemination of scientific research documents, whether they are published or not. The documents may come from teaching and research institutions in France or abroad, or from public or private research centers.

L'archive ouverte pluridisciplinaire **HAL**, est destinée au dépôt et à la diffusion de documents scientifiques de niveau recherche, publiés ou non, émanant des établissements d'enseignement et de recherche français ou étrangers, des laboratoires publics ou privés.



Distributed under a Creative Commons Attribution 4.0 International License

1 Unravelling Platinum-Zirconia Interfacial Sites 2 using CO Adsorption.

3 *Frederic C. Meunier**, Raphael Kdhir, Natalia Potrzebowska, Noémie Perret, Michèle Besson,
4 *Univ Lyon, Université Claude Bernard Lyon 1, CNRS, IRCELYON, 2 Av. Albert Einstein, 69626*
5 *Villeurbanne (France).*

6 **KEYWORDS:** CO adsorption; platinum; FT-IR; DRIFTS; multi-bonded carbonyl.

7
8 **ABSTRACT:** Understanding platinum speciation on catalysts is crucial for the design of atom-
9 efficient materials and optimized formulations. The adsorption of CO as probe molecule is
10 widely used to reveal Pt dispersion and structures, yet the assignment of IR bands is not
11 straightforward, hindering the determination of the nature of the surface sites or ensemble
12 involved. CO adsorption was studied here over a zirconia-supported Pt catalyst. Specific sites at
13 the interface between Pt and the support were highlighted giving rise to an unusual band around
14 1660 cm^{-1} that could be confidently assigned to a Pt₂-CO bridging carbonyl interacting head-on
15 with a support surface hydroxyl. This adduct was yet unstable in the present conditions and was
16 converted into linear and bridged carbonyl only bound to Pt. Such sites are potentially important
17 for bifunctional reactions requiring both metal and acid/base properties, particularly those
18 occurring at the metal - support perimeter. Such adducts have probably been mistaken for

1 carbonate-type species in many past contributions and could potentially represent crucial
2 reaction intermediates for CO oxidation and the water-gas shift reaction.

3

4 **1. Introduction**

5

6

7 Pt-based materials are widely used in heterogeneous catalysis and electrochemistry.

8 Understanding metal speciation is crucial for the design of atom-efficient materials and

9 optimized formulations^{1,2,3}. The adsorption of CO as a probe molecule is widely used as a means

10 to determine Pt structures, by interpreting the value of the C-O bond stretching frequency $\nu(\text{CO})$

11 in the adsorbed state. Yet, the assignment of IR bands is not always straightforward, hindering

12 the determination of the nature of the surface sites present.

13 The difficulty in interpreting IR spectra related to CO adsorption on platinum-based surfaces

14 and catalysts has long been discussed.⁴ The stretching frequency $\nu(\text{CO})$ is affected, among

15 others, by the nature (e.g. coordination number, oxidation state) of the Pt sites present, CO

16 adsorption modes and lateral interactions between adsorbed CO (so called “dipole-dipole

17 coupling”).

18 Lateral interactions imply band intensity transfer that can make spectral interpretation difficult,

19 even at low surface coverage if island formation takes place.^{5,6} Lateral interactions were shown

20 to be markedly decreased in the case of intermetallic Pt-Sn nanoalloys, in which Pt atoms are

21 spatially separated by Sn atoms.⁷ The wavenumber of $\nu(\text{CO})$ free of dipole-dipole interaction is

22 otherwise determined by using isotopically labelled mixtures of ^{12}CO and ^{13}CO , which exhibit a

23 wavenumber ratio of $\nu(^{12}\text{CO}) / \nu(^{13}\text{CO}) = 1.023$. The ca. 50 cm^{-1} wavenumber difference is

1 sufficient to decouple these electrodynamic vibrators and obtain the so-called “singleton” value
2 for the diluted isotopomer.⁴

3 The coordination number (C.N.) of the Pt atoms affects dramatically the wavenumber of the
4 stretching vibration of the adsorbed CO. Kappers and van der Maas⁸ reported a linear correlation
5 between the wavenumber of linearly adsorbed CO and Pt coordination number, ranging from
6 1996 cm^{-1} (C.N. = 3, Pt adatom) up to 2096 cm^{-1} (C.N. = 9, Pt in (111) plane). These
7 assignments were based on a few assumptions, including a cubo-octahedral shape for the Pt
8 crystals (from which the proportion of sites with a given coordination can be determined)⁹ and a
9 complex band decomposition based on second derivatives.

10 The oxidation state of Pt strongly affects the position of the CO band. While CO adsorbed on
11 metallic sites typically exhibit wavenumbers lower than 2096 cm^{-1} , Hadjiivanov and co-workers
12 showed that (single atom) cationic Pt in zeolite-based materials absorb at much higher
13 wavenumbers.^{10,11,12} Pt^{3+} cations were shown to form $\text{Pt}^{3+}(\text{CO})_2$ dicarbonyls leading to doublets,
14 with high and low wavenumber bands ranging from 2211 to 2195 cm^{-1} and from 2175 to 2155
15 cm^{-1} , respectively. In the case of Pt^{2+} , both mono and dicarbonyls were observed. Pt^{2+} -CO
16 species were absorbing typically over the range 2155-2141 cm^{-1} , while the $\text{Pt}^{2+}(\text{CO})_2$ dicarbonyls
17 exhibiting a doublet at 2165 and 2150 cm^{-1} . In the case of Pt^+ , monocarbonyl Pt^+ -CO (ca. 2112
18 cm^{-1}), dicarbonyls $\text{Pt}^+(\text{CO})_2$ (2135-2120 and 2101-2091 cm^{-1}) and tricarbonyls $\text{Pt}^+(\text{CO})_3$ (2162,
19 2150 and 2110 cm^{-1}) were proposed. These authors also proposed that supported Pt^{4+} ions are
20 coordinatively saturated and not able to form carbonyls after CO adsorption.

21 CO adsorption on single atom Pt species has also been reported on other traditional non-
22 zeolitic oxide supports. Single atom Pt species, presumably Pt^{2+} , supported on ceria lead to bands
23 around 2090 cm^{-1} .^{13,14} Stair and co-workers assigned bands around $2105 \pm 10 \text{ cm}^{-1}$ to positively

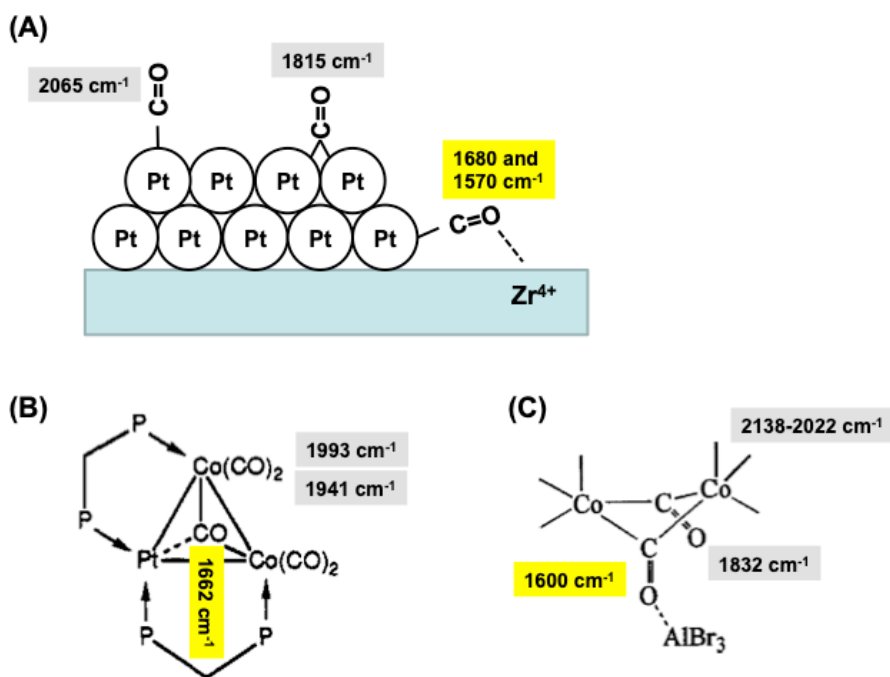
1 charged single atom Pt present on silica, alumina and titania.¹ The band was located around 2090
2 $\pm 10 \text{ cm}^{-1}$ in the case of zirconia. The CO adsorbed on single atom species could be
3 discriminated from those adsorbed on Pt nanoparticles by the fact that the latter were removed
4 through oxidation by O_2 even at room temperature, while the CO adsorbed on single atoms were
5 unreactive at low temperatures.

6 The mode of binding of CO affects markedly $\nu(\text{CO})$. Surface science data collected by
7 Hayden and Bradshaw on Pt(111) surfaces between at 85–300 K reported on-top (linearly
8 adsorbed) CO at 2110 cm^{-1} , two-fold bridge CO at 1842 and three-fold bridge CO at 1822 cm^{-1} .¹⁵
9 Note that the 2110 cm^{-1} value for linear species absorption is significantly higher than the value
10 expected for CO adsorbed on metallic Pt atom with a C.N. = 9, which is 2096 cm^{-1} as proposed
11 by the model of Kappers and van der Maas.⁸ This difference is probably due to the occurrence of
12 dipole-dipole effects in the case of the data reported on Pt(111) leading to a large increase of the
13 wavenumber value.

14 Heterobridging CO species have been proposed by a number of teams. CO bridged between Pt
15 and sites of the alumina support that adsorbed at 1756 cm^{-1} were proposed by Ferri et al.¹⁶ Dilara
16 and Vohs assigned bands located at 1680 and 1570 cm^{-1} to a head-and-tail CO adduct formed
17 between Pt and a Zr^{4+} cation, while linear and bridged CO solely adsorbed on Pt adsorbed at
18 2065 and 1815 cm^{-1} , respectively (Fig. 1.A).¹⁷ Carbonyl coordination complexes of various
19 metals exhibit bands at low wavenumbers, such as 1662 cm^{-1} assigned to a “semitriple bridging”
20 carbonyl in $\text{PtCo}_2(\text{CO})_5(\mu\text{Ph}_2\text{P-CH}_2\text{-PPh}_2)$ (Fig. 1.B).¹⁸ The formation of adducts through the
21 oxygen atom of CO interacting with Lewis centre can decrease $\nu(\text{CO})$ by as much as 232 cm^{-1} , as
22 in the case of $\text{Co}_2(\text{CO})_8$ and its adduct with AlBr_3 (Fig. 1.C).¹⁹ The wavenumber of the bridging

1 carbonyl forming the adduct was 1600 cm^{-1} , as compared to 1832 cm^{-1} for the parent bridged
2 species.

3



4

5 Figure 1: Example of heterobonding carbonyl species proposed in the literature and the
6 corresponding wavenumbers of the C-O bond stretching mode (highlighted in yellow). Common
7 on-top and bridged carbonyl species are also depicted. Adapted from various references.^{17,18,19}

8

9 The formation of carbonates and hydrogenocarbonates should always be considered when
10 adsorbing CO on catalyst surfaces because of the presence of residual traces of CO_2 or its
11 formation *in situ* through various reactions that are easily catalyzed by metals, e.g. Boudouard ($2\text{ CO} \rightarrow \text{C} + \text{CO}_2$), water-gas shift ($\text{CO} + \text{H}_2\text{O} \rightarrow \text{H}_2 + \text{CO}_2$) and oxidation with oxygen supplied
12 by residual dioxygen or the catalyst ($\text{CO} + \text{O} \rightarrow \text{CO}_2$). Surface carbonates typically exhibit two
13 bands between 1700 and 1100 cm^{-1} , resulting from the splitting of the ν_3 band (asymmetric CO_3
14 stretching) at 1415 cm^{-1} of the free carbonate ion, which exhibits D_{3h} symmetry.²⁰ The
15

1 wavenumber difference between the two bands ($\Delta\nu_3$) depends on the carbonate coordination
2 mode,²¹ but also on the charge and radius of the cation it is adsorbed on.²² Monodentate
3 carbonate can exhibit $\Delta\nu_3$ as low as 60 cm^{-1} (e.g. 1460 and 1400 cm^{-1} on $\alpha\text{-Fe}_2\text{O}_3$),²³ while
4 bidentate and bridged carbonate can present $\Delta\nu_3$ above 300 cm^{-1} (e.g. 1610 and 1290 cm^{-1} on $\alpha\text{-}$
5 Fe_2O_3)²³.

6 Newton et al.²⁴ assigned the signal of a single band located at 1690-1670 cm^{-1} observed over
7 alumina-supported Pt to a Pt carbonate species. This band was shown to be a crucial reaction
8 intermediate in the formation of CO_2 during $\text{CO} + \text{O}_2$ reaction using a combination of *operando*
9 DRIFTS and mass spectrometry data. The assignment of this band to a carbonate may yet be
10 questioned in view of the aforementioned discussion.

11 Hydrogenocarbonates are typically formed from the reactive adsorption of CO_2 on surface
12 hydroxyl groups²⁵ and the characteristic IR bands at the surface of ZrO_2 are located at 1625
13 ($\nu_a(\text{CO}_3)$), 1425 ($\nu_s(\text{CO}_3)$) and 1222 ($\delta(\text{OH})$) cm^{-1} .²⁶ Carboxylates (i.e. CO_2 adsorbed on a metal
14 centre) also typically present a pair of bands between 1700 and 1200 cm^{-1} .²²

15 We are revisiting here the speciation of Pt supported over a zirconia support. Pt/ ZrO_2 and
16 Pt/sulfated- ZrO_2 catalysts have raised a lot of interest for a wide range of important reactions
17 such as water-gas shift²⁷, methane dry reforming²⁸, aqueous phase selective oxidation²⁹ and
18 reforming³⁰ of biomass-derived compounds, room temperature oxidation of formaldehyde³¹ and
19 CO ³², electrooxidation of alcohols^{33,34} and alkane isomerization^{35,36}. The speciation of Pt over
20 zirconia using CO as molecular probe was investigated and revealed a variety of sites ranging
21 from isolated Pt atoms to large Pt particles. Specific sites at the interface between Pt and the
22 ZrO_2 support were also highlighted. These interfacial sites exhibited yet a limited stability in the
23 present conditions. Such sites are potentially important for bifunctional reactions requiring both

1 metal and acid/base properties, particularly those thought to be occurring at the metal - support
2 perimeter.

3

4 **2. Experimental Section**

5

6 The zirconia supplied by MEL Chemicals (XZO 632-18) exhibited a surface area of $136 \text{ m}^2 \text{ g}^{-1}$.
7 ¹. The Pt precursor hexachloroplatinic acid ($\text{H}_2\text{PtCl}_6, 6 \text{ H}_2\text{O}$ 99.9%) was bought from Alfa Aesar,
8 NaBH_4 was purchased from Acros Organics. The zirconia-supported Pt was prepared by wet
9 impregnation using NaBH_4 as the reducing agent. The support (ca. 5 g) and deionized water (250
10 mL) were introduced in a 1 L round-bottom flask. The appropriate volume of an aqueous
11 solution of H_2PtCl_6 (containing $14.4 \text{ g}_{\text{Pt}} \text{ L}^{-1}$) was added and the impregnation took place under
12 moderate stirring in an ultrasound bath (37 kHz) for 3 h. After cooling to ca. 10°C with an ice
13 bath, a freshly prepared NaBH_4 solution (0.73 g in 50 mL deionized water) was slowly added
14 under vigorous stirring. The suspension immediately turned to black and was stirred for an
15 additional 2 h. The solid was filtered, washed with water, and dried at 60°C under nitrogen
16 overnight. The Pt loading was measured by Inductively Coupled Plasma-Optical Emission
17 Spectrometry (ICP-OES, Jobin Yvon Activa) after mineralization of the solid. The Pt loading
18 measured was 2.2 wt%.

19 Powder X-ray diffraction patterns were recorded on a Bruker D8 Advance A25 diffractometer
20 using $\text{Cu K}\alpha$ radiation ($\lambda = 0.1541 \text{ nm}$) in the range between $2\theta = 20 - 60^\circ$ at a step of $0.02^\circ \text{ s}^{-1}$.

21 The crystalline phases were identified by reference to the JCPDS files.

1 The TEM images were obtained using a JEOL 2010 microscope with LaB6 source operated at
2 200 kV. The sample was suspended in EtOH solution and a drop of the sonicated suspension was
3 deposited onto carbon-coated Cu grid and solvent was evaporated.

4 High purity gases He (99.999%) and CO (99.9%) from Air Liquid were used. The gases were
5 further purified using a liquid nitrogen trap located just before the DRIFTS cell to remove traces
6 of water, CO₂ and hydrocarbons.

7 DRIFTS experiments were performed at 50°C with a modified high temperature DRIFT cell
8 (from Spectra-Tech) fitted with KBr windows, using a DRIFT-II assembly. A description and
9 properties of the cell can be found in earlier references.^{37,38} The spectrophotometer used was a
10 Nicolet 6700 (ThermoFischer Scientific) fitted with a liquid-N₂ cooled MCT detector. The
11 DRIFT spectra were recorded at a resolution of 4 cm⁻¹ and 32 scans were averaged. The
12 DRIFTS spectra are reported as log (1/R), where R is the sample reflectance. This pseudo-
13 absorbance gives a better linear representation of the band intensity against surface coverage
14 than that given by the Kubelka-Munk function for strongly absorbing media such as those based
15 on metals supported on oxides.³⁹ The contribution of gas-phase CO was subtracted using a
16 CO(g) spectrum collected under the same experimental condition over KBr powder.

17

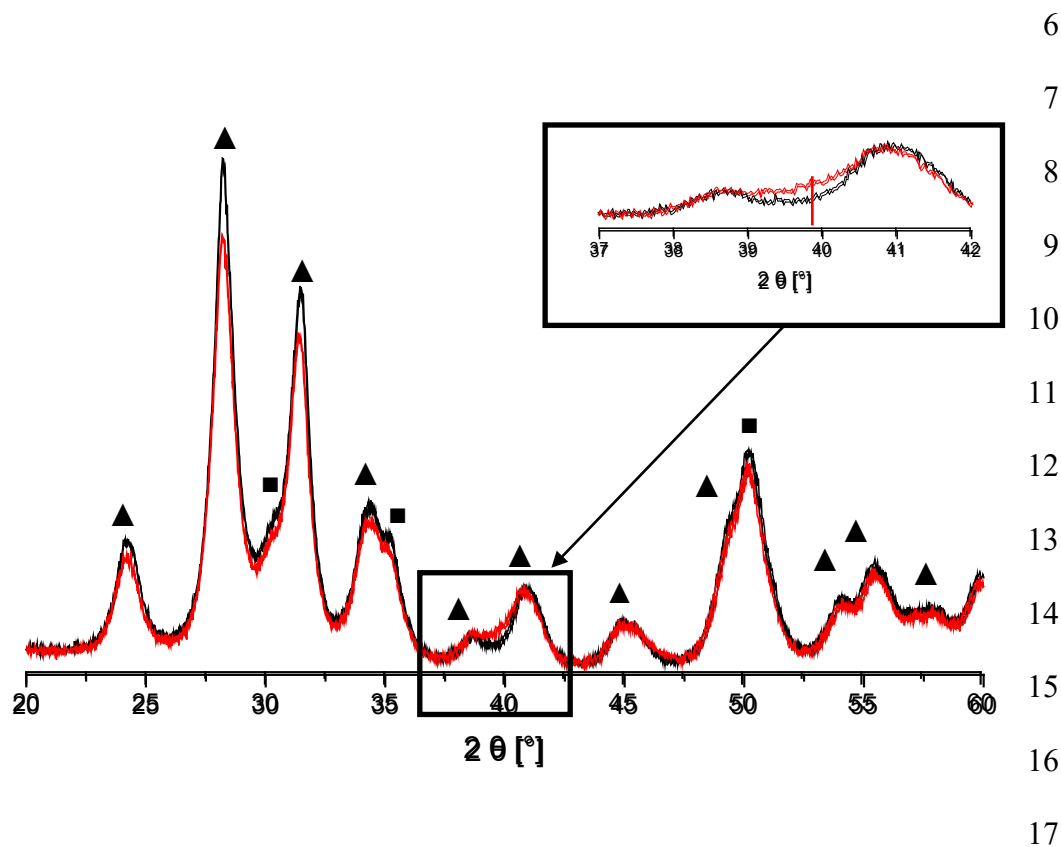
18 **3. Results**

19 **3.1. Sample characterization**

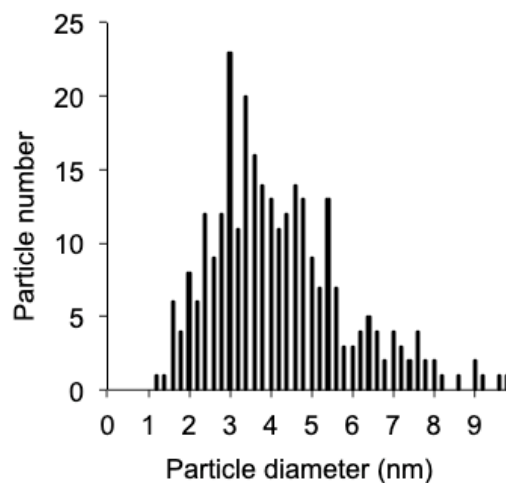
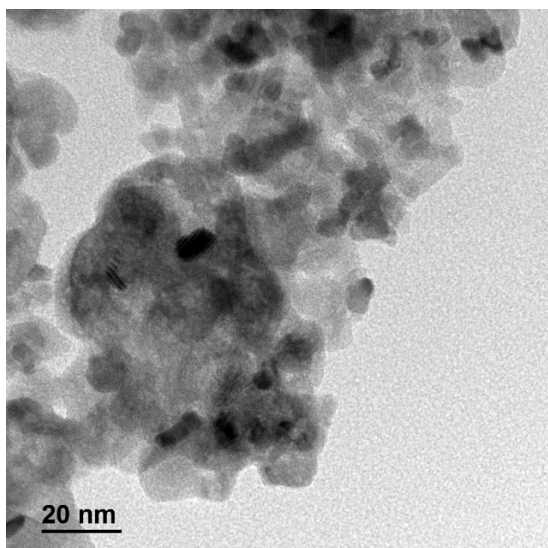
20

21 The XRD patterns of the zirconia support and Pt/ZrO₂ solid are shown in Fig. 1. The support
22 sample showed intense peaks indexed to the monoclinic phase (JCPDS 00-037-1484). The
23 pattern also showed peaks associated with the tetragonal phase (JCPDS 01-80-0965). The ratio

1 of $m\text{-ZrO}_2$ / $t\text{-ZrO}_2$ is of 90%/10%, as determined by Rietveld refinement, using the Topas 5
2 software. The XRD pattern of the material containing 2.2 wt.% Pt was essentially identical,
3 excepted for a weak and wide peak at ca. $2\theta = 39.9^\circ$ associated with the (111) plane of cubic Pt
4 (Fig. 1, inset in the region between 37 and 43°).
5



18
19 **Figure 1.** XRD patterns of bare ZrO_2 and Pt/ZrO_2 . The peaks corresponded to: monoclinic
20 ZrO_2 JCPDS 00-037-1484 (▲), tetragonal ZrO_2 JCPDS 01-80-0965 (■) and Pt JCPDS 00-004-
21 0802.
22
23

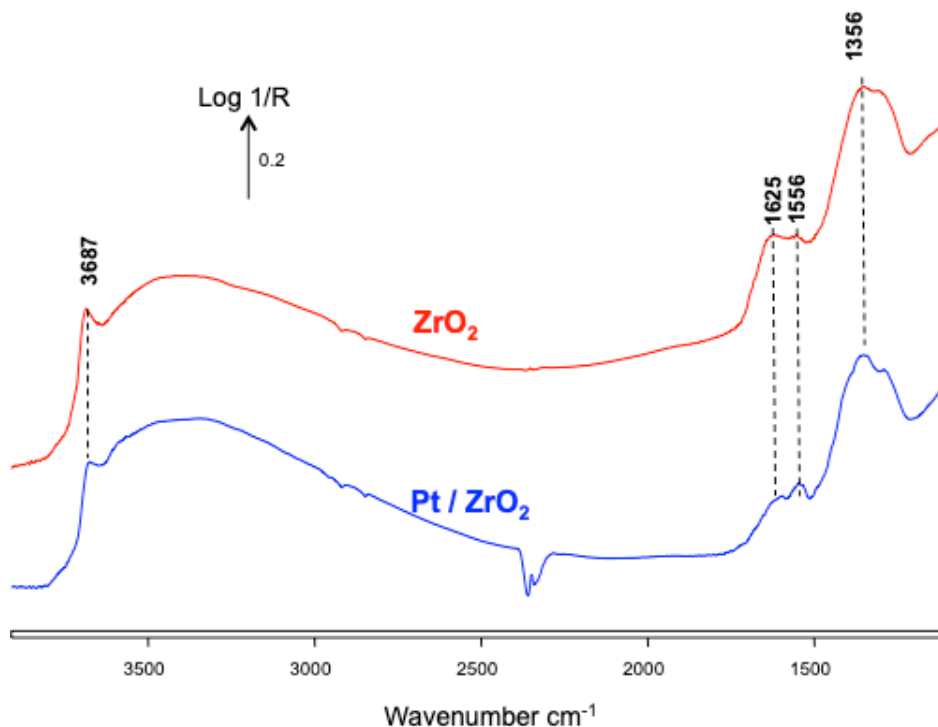


4 **Figure 2.** TEM picture of the Pt/ZrO₂ catalyst and the corresponding distribution of Pt particle sizes.

5 The Pt particle size distribution measured by TEM counting about 200 particles is given in Fig.
6 2. Most Pt particles were comprised between 2 and 6 nm in diameter, with a mean particle size of
7 4.5 nm leading to Pt dispersion of about 22%.

8 The DRIFTS spectra of the ZrO₂ support and Pt/ZrO₂ heated for 30 min in He at 50°C were
9 similar in nature (Fig. 3). Though the commercial zirconia used was not sulfated, evident bands
10 centered around 1356 cm⁻¹ were observed and corresponded to ZrO₂-bound sulfate species.^{40,41}
11 Bands in the 3800-2500 cm⁻¹ region corresponded to various free and H-bonded hydroxyl
12 groups. The bands at 1625 and 1556 cm⁻¹ can be assigned to the overlap of various bands
13 associated with adsorbed water and carbonate species.

14

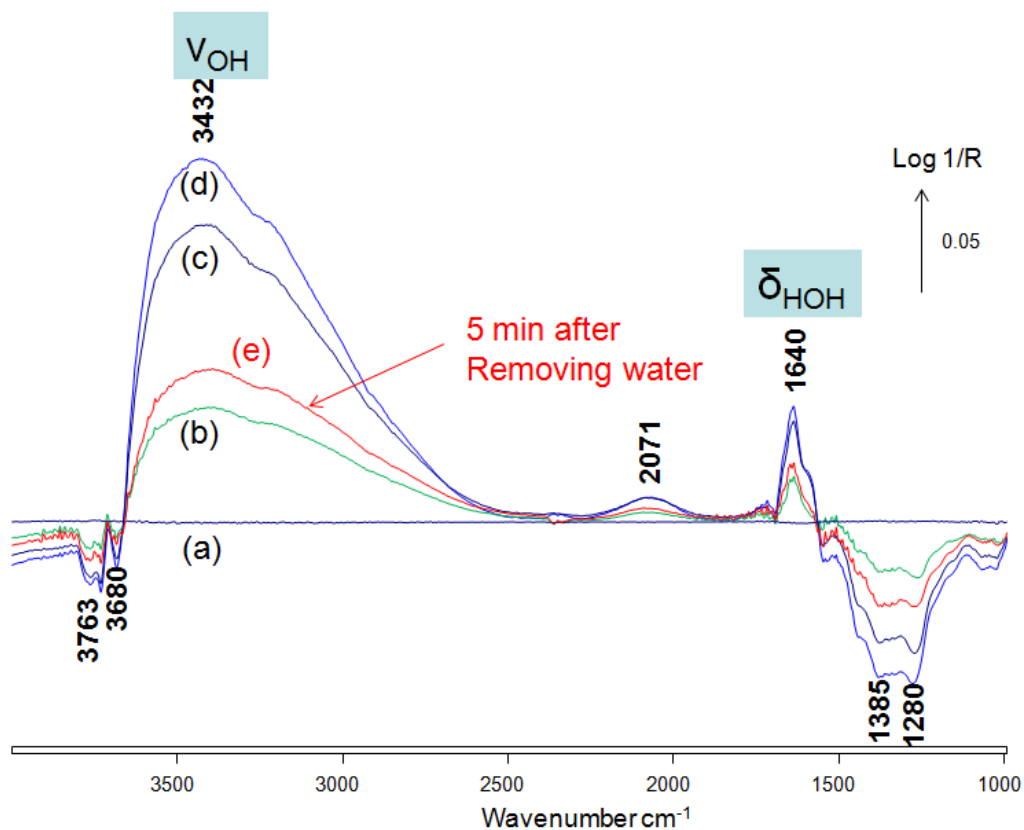


1
2 **Figure 3.** DRIFTS spectra of ZrO₂ and Pt/ZrO₂ recorded at 50°C after 1h in He. KBr signal
3 was used as background.

5 3.2. Water adsorption on ZrO₂

6 The effect of the addition of water was investigated over the ZrO₂ support. Water was
7 added by passing the He stream into a water-filled saturator kept at 0°C. The presence of water
8 resulted in the formation/increase of several IR bands as well as the displacement of bands
9 previously present (Fig. 4). The 1640 cm⁻¹ band corresponded to the bending mode of adsorbed
10 water. The large band with a maximum at 3432 cm⁻¹ was due to the stretching modes of adsorbed
11 water and surface hydroxyls, both being hydrogen-bonded, also resulting in the displacement of
12 hydroxyl groups previously present at 3763 and 3680 cm⁻¹ towards lower wavenumbers. The
13 2071 cm⁻¹ is a band associated with surface hydroxyls and water, so-called Evan's windows, due
14 to Fermi resonance between hydroxyl vibration modes. The negative bands at 1385 and 1280 cm⁻¹

1 ¹ were due to the perturbation of sulfate groups by water. All these changes were gradually
2 reversed once water was removed from the feed (Fig. 4.e).

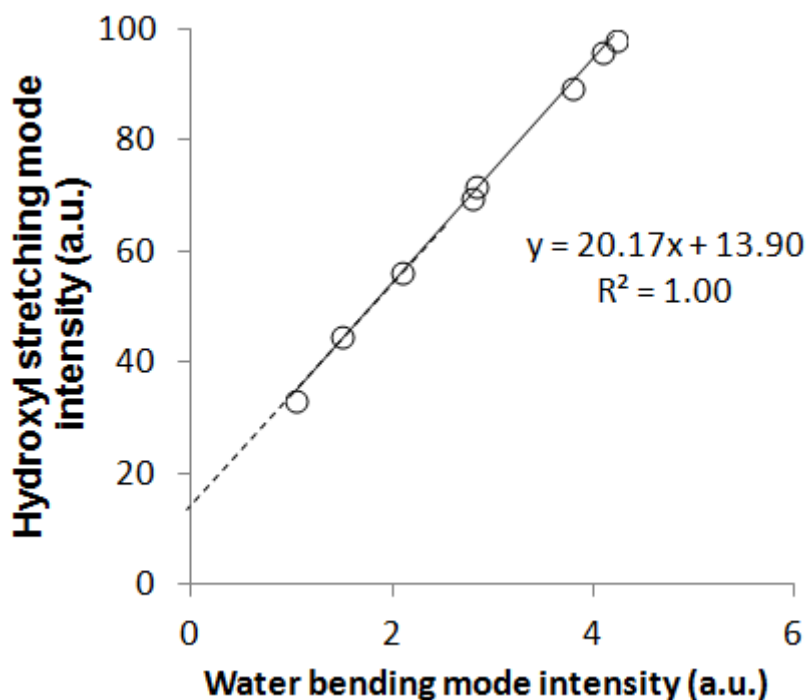


3
4 **Figure 4.** Examples of DRIFTS spectra of the support ZrO₂ at 50°C under 30 mL min⁻¹ of He
5 recorded (a-d) over a 10 min period following the introduction of 0.6 kPa of water and (e) 5 min
6 after removing water. The DRIFTS signal collected over the sample dried for 30 min at 50°C
7 under He was used as background.

8
9 The signal of the hydroxyl stretching bands formed during water adsorption exhibited a linear
10 correlation with that of water bending mode (Fig. 5). The line offset was likely due to the
11 dissociative adsorption of water over Zr-O-Zr oxo-bridges and sulfone S=O groups, which led to
12 the formation of new hydroxyl groups without any corresponding signal from water bending

1 mode. The slope of the line indicate that the molar absorption coefficient of the –OH stretching
2 band was ca. 20-fold higher than that of water bending mode.

3



4

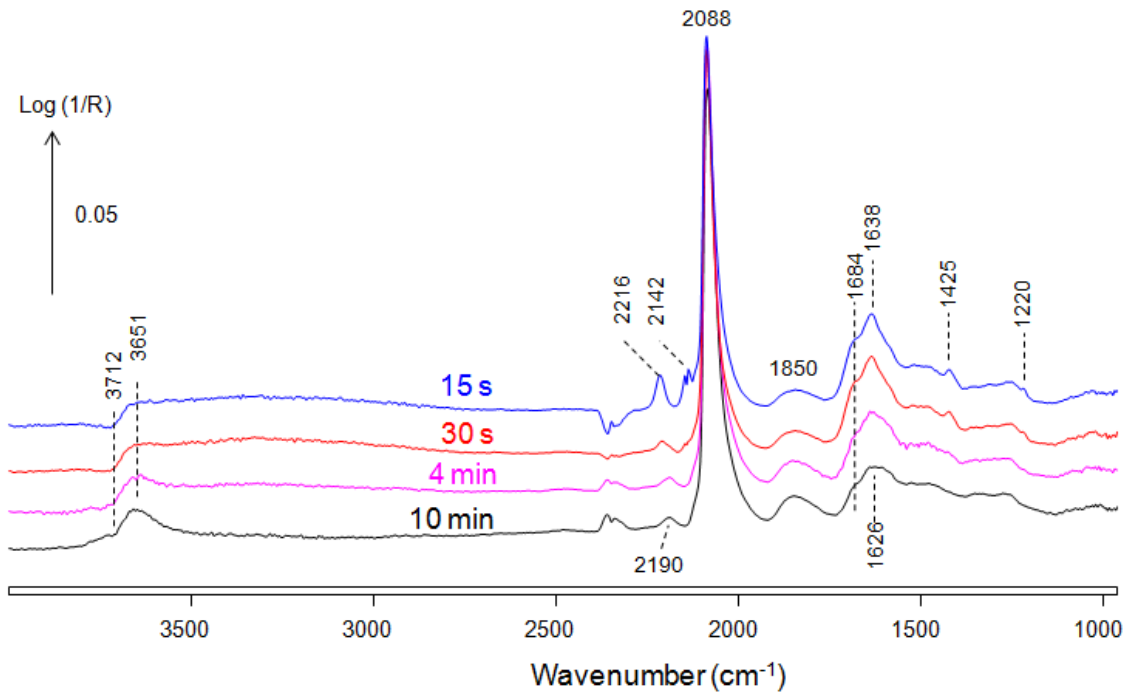
5 **Figure 5.** Evolution of the intensity of the DRIFTS signal of the hydroxyl stretching bands
6 (integrated over 3647-2500 cm^{-1}) versus that of water bending mode (integrated over 1690-1576
7 cm^{-1}) during water uptake at 50°C.

8

9 **3.3. CO adsorption**

10 The samples were investigated without applying any *in situ* pre-treatment apart from
11 stabilizing the sample in He for 1 h at 50°C. CO adsorption was then monitored at 50°C. No
12 band formation could be detected in the case of the bare support (data not shown). In contrast,
13 many bands were formed on the Pt/ZrO₂.

14



1
2 **Figure 6.** DRIFTS spectra collected over the Pt/ZrO₂ at 50°C under 3% CO/He at various
3 times following CO introduction. The sample spectrum collected under He before CO
4 introduction was used as background. The gas-phase spectrum of CO was subtracted.

5
6 The main band observed over the Pt/ZrO₂ following CO introduction was located at 2088 cm⁻¹
7 (Fig. 6 and Table 1) and corresponded to CO linearly adsorbed on Pt atoms with high
8 coordination numbers as present in the terraces of the nanoparticles (Fig. 2). The asymmetric
9 shape of the band and the tail towards lower wavenumbers down to 1970 cm⁻¹ was associated
10 with CO linearly adsorbed on sites with lower coordination numbers and smaller nanoparticles.
11 The band located at 1850 cm⁻¹ is assigned to bridged CO adsorbed on metallic Pt.

12 A doublet was initially visible at 2216 and 2142 cm⁻¹ that is likely assigned to geminal CO
13 adsorbed on oxidized Pt sites (Fig. 6 and Table 1). The intensity of this doublet rapidly decreased
14 within the first 30 s of exposure to CO, suggesting that some of the oxidized Pt was getting
15 reduced in the presence of CO, thereby releasing some CO₂. The CO₂ evolved was responsible

1 for the formation of minor bands due to hydrogenocarbonates at ca. 1638+1425+1220 cm⁻¹,
 2 which had then vanished after 4 min. A weak band at 2190 cm⁻¹ remained, likely due to CO
 3 linearly adsorbed on some still oxidized Pt.

4

5 **Table 1.** IR band assignment related to ¹²CO (and ¹³CO, in brackets) adsorption. “L” refers to
 6 linearly adsorbed CO and “B” to bridged CO between two Pt atoms. The wavenumber ratio
 7 between gas-phase ¹²CO and ¹³CO is 1.023.

8

Wavenumber (cm ⁻¹)	¹² CO/ ¹³ CO wavenumber ratio		References
2216 + 2142	n.d.	Pt ³⁺ -(CO) ₂	10,11,12
2190 (2135)	1.026	L-CO on Pt ³⁺	10,11,12
2088 (2032)	1.028	L-CO on Pt ⁰	4,8
1850 (1794)	1.031	B-CO on Pt ⁰	15
1684	n.d.	B-CO····HO-	This work
1626 (1586)	1.025	B-CO····HO-	This work
1700 - 1200	n.d.	Various carboxylates and carbonates	22,23
1638 + 1425 + 1220	n.d.	hydrogenocarbonate	26

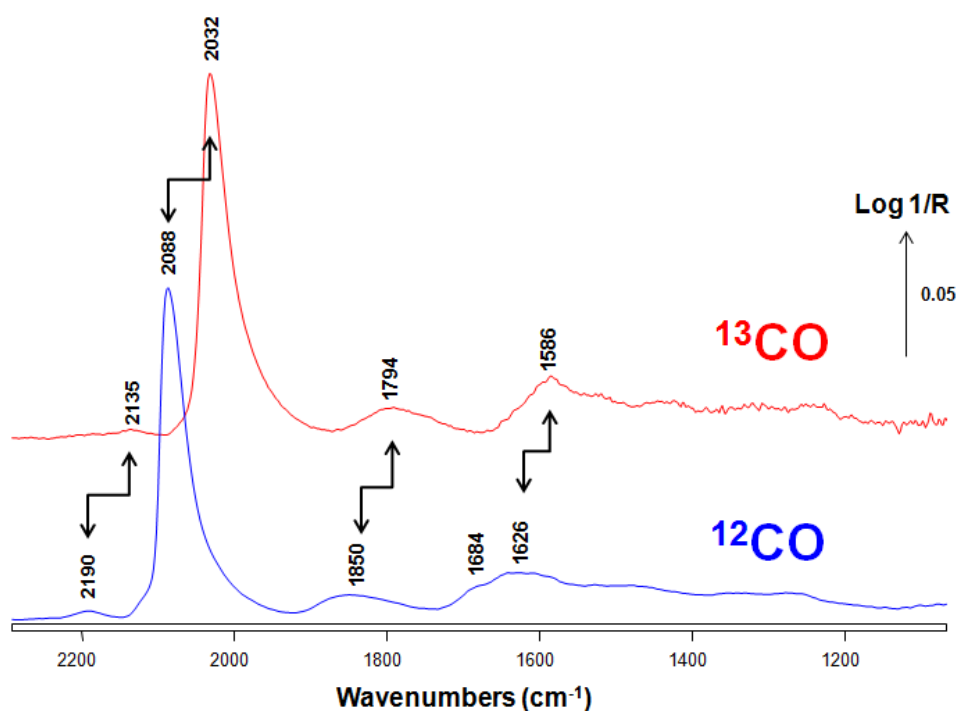
9
10

11 A continuum of ill-defined bands was observed between 1750 and 1200 cm⁻¹ after the
 12 disappearance of the hydrogenocarbonate bands (Fig. 6, 10 min). The most prominent band was
 13 located at 1626 cm⁻¹, also exhibiting a shoulder at 1684 cm⁻¹. Bands at these positions can be
 14 possibly related to (i) adsorbed molecular water, (ii) carbonates or (iii) multibonded CO.

15 Assigning the rather large 1626 and 1684 cm⁻¹ bands to adsorbed molecular water can be
 16 confidently excluded in view of the corresponding very weak signal observed in the region 3800-
 17 2500 cm⁻¹ (Fig. 6), in contrast to the proportions expected when these bands are due to water O-

1 H stretching and H-O-H bending modes, respectively (Fig. 4). A band at 3651 cm^{-1} was probably
2 due to the perturbation of the missing hydroxyl at 3712 cm^{-1} by adsorbed species.

3 An additional experiment using ^{13}CO was carried out to confirm that the bands at 1626 and
4 1684 cm^{-1} were not due to water. The spectrum obtained using ^{13}CO led to the expected band
5 redshift of ca. 50 cm^{-1} for all the bands assigned to carbonyl species (Fig. 7), corresponding to
6 the theoretical wavenumber ratio of $^{12}\text{CO}/^{13}\text{CO}$ of 1.023 within experimental error (Table 1). In
7 particular, the bands at 1626 and 1684 cm^{-1} were clearly redshifted by the expected value
8 (though the high wavenumber shoulder was not visible in the ^{13}CO spectrum), confirming that
9 these bands were related to an adsorbate containing a C-O bond of some order and not to water.

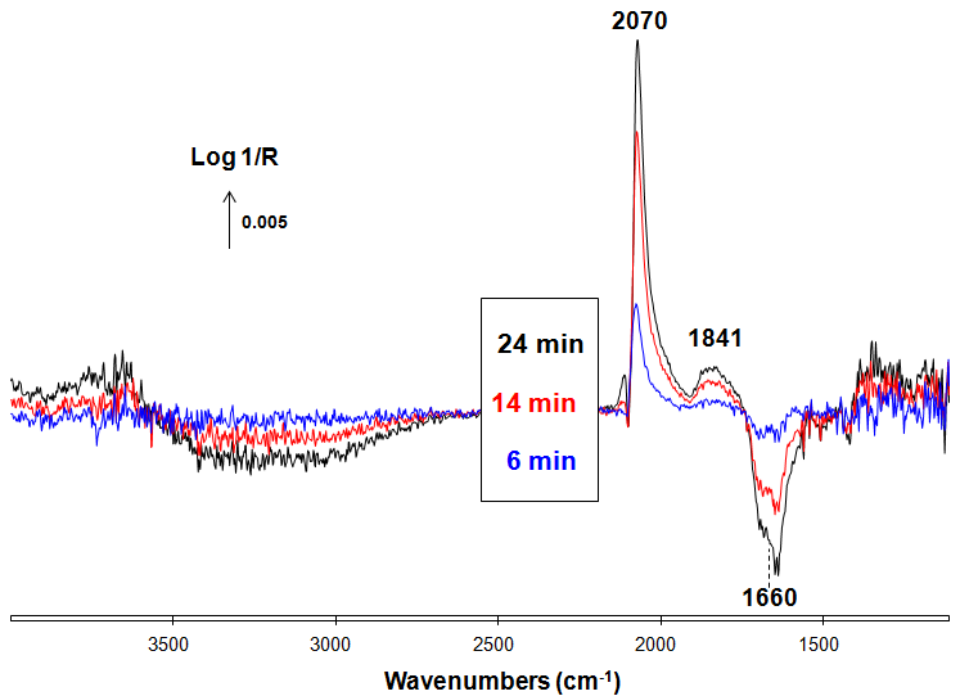


10

11 **Figure 7.** DRIFTS spectra collected over the Pt/ZrO₂ at 50°C under 3% CO/He at after 10 min
12 following ^{12}CO or ^{13}CO introduction. The spectrum of the sample at the same temperature
13 collected under He before CO introduction was used as background. The gas-phase spectrum of
14 CO was subtracted.

1
2
3
4
5
6
7
8

The evolution of the DRIFTS spectra with time under CO were monitored using the spectrum collected at 4 min as reference, since it corresponded to the time at which most oxidized Pt had been reduced and hydrogenocarbonate bands were no longer visible (Fig. 6). The intensity of the broad band centered at 1660 cm^{-1} , which encompassed those at 1626 and 1684 cm^{-1} , clearly decreased (Fig. 8). In contrast, the bands at 2070 and 1841 cm^{-1} , corresponding to linear and bridged CO adsorbed on Pt, increased.

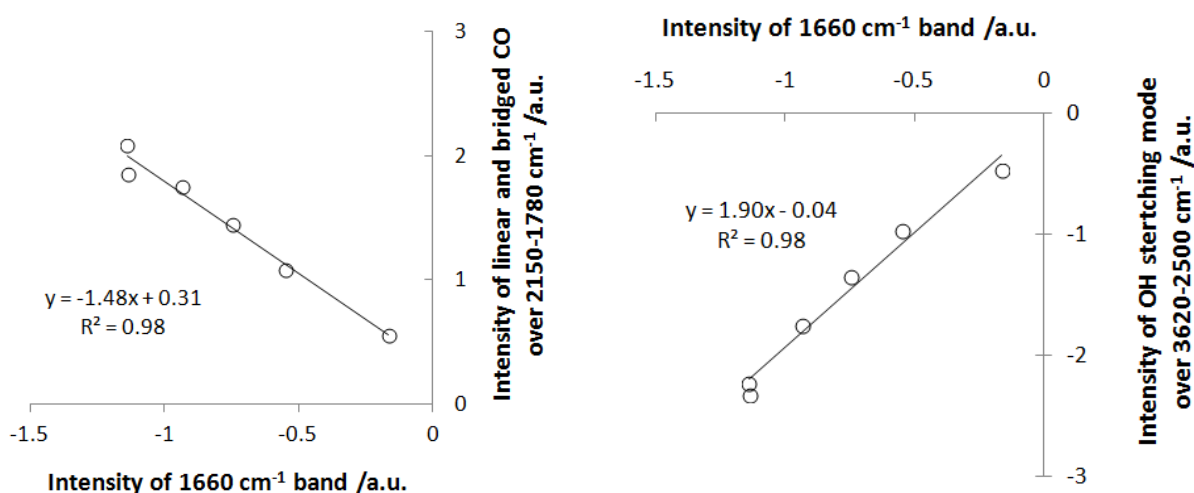


9
10
11
12
13

Figure 8. Typical DRIFTS spectra collected over the Pt/ZrO₂ at 50°C under 3% CO /He at various times following CO introduction. The spectrum collected after 4 min was used as background. The gas-phase spectrum of CO was subtracted.

1 A linear correlation was noted when plotting the area of the linear and bridged bands as a
2 function of the intensity of the 1660 cm^{-1} band (Fig. 9, Left). This suggests that vanishing species
3 corresponding to the 1660 cm^{-1} band was quantitatively converted into linear and bridged CO
4 adsorbed on Pt.

5 Similarly, the signal in the $3620\text{-}2500\text{ cm}^{-1}$ region corresponding to hydroxyl stretching
6 vibration modes decayed linearly with respect to the band intensity at 1660 cm^{-1} (Fig. 9, Right).
7 The slope of the line was far lower than that expected when describing the relation between
8 water bending mode and water hydroxyl stretching modes as described in Fig. 4 and 5.
9 Therefore, the observed decaying signals observed in Fig. 8 were not, in most part, the result of
10 water desorption from the sample.



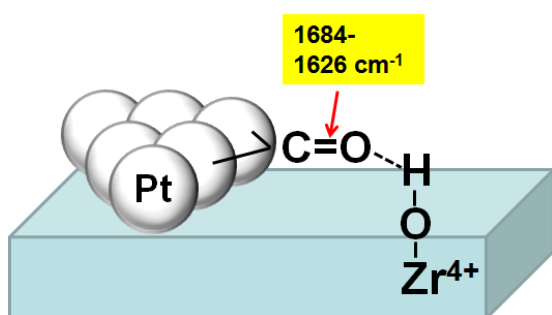
11
12 **Figure 9.** Integration of DRIFTS bands relating to the data reported in Fig. 8. (Left) Area of
13 the DRIFTS band of the linear and bridged CO as a function of that of the 1660 cm^{-1} band.
14 (Right) Area of the DRIFTS band of hydroxyl groups as a function of that of the 1660 cm^{-1} band.
15 The band at 1660 cm^{-1} was integrated over the range $1780\text{-}1560\text{ cm}^{-1}$.
16

1 A possible explanation for the behavior observed in Fig. 8 and 9 is that the bands around 1660
2 cm^{-1} (i.e. ranging from 1684 to 1626 cm^{-1} in Fig. 6) represented CO adsorbed on Pt metallic
3 atoms, bridging with a surface hydroxyl group from the support, as represented in Fig. 10. The
4 wavenumber range is consistent with those reported earlier for multibonded CO, notably those
5 involving bonds between the surface and both C and O atoms (Fig. 1.A and 1.C and references
6 17,19). In the present case, this adduct is not stable and the bonding between CO and the surface
7 hydroxyl is gradually lost, possibly due to a rearrangement of the corresponding Pt nanoparticles.
8 New linear and bridging carbonyls are then formed, which do not interact with the support, as
9 suggested by the data reported in Fig. 8.

10 We can reasonably exclude that the bands around 1660 cm^{-1} were due to some carbonate
11 species, because of the lack of additional bands at lower wavenumbers (Fig. 8), which are
12 expected when the doubly degenerated asymmetric stretching modes of the D_{3h} carbonate ion at
13 1415 cm^{-1} splits upon symmetry loss²².

14 It is therefore possible that single bands observed in other cases in this region may be due to
15 this peculiar bridging carbonyl. The single band at 1670-1690 cm^{-1} reported by Newton and co-
16 workers²⁴ on alumina-supported Pt, which the authors assigned to a carbonate adsorbed on Pt,
17 may actually be a similar type of carbonyls bridging between Pt and alumina. It must be stressed
18 that the disappearance of this band was also mirrored by the appearance of both bridged and
19 linear CO adsorbed on Pt (Fig. 3.A in reference 24), exactly as we observed here (Fig. 8).
20 Unfortunately, the OH stretching region was not shown, so it is not clear whether a change in
21 OH signal also occurred in their case. Resolving the nature of this band is important because it
22 appeared to be the intermediate species leading to CO_2 formation during the oxidation of CO
23 with O_2 at room temperature²⁴.

1 A direct characterization of this species is yet tedious as shown here because of the many other
2 species (water, carbonate, hydrogenocarbonate) that may give rise to IR bands in this region too.
3 This species may actually be the one already reported by Dilara and Vohs¹⁷, which was assigned
4 to interfacial sites without mentioning the involvement of surface hydroxyl groups. Such sites are
5 potentially important for bifunctional reactions requiring both metal and acid/base properties,
6 particularly those thought to be occurring at the metal - support perimeter. Such adducts formed
7 between Pt and hydroxylated supports could potentially represent crucial reaction intermediates
8 for the CO oxidation and the water-gas shift reaction.^{2,24,42}



10
11 **Figure 10.** Schematic representation of a bridging carbonyl bound to Pt atoms and interacting
12 head-on with the support surface hydroxyl groups, leading to low C=O wavenumbers in the
13 range 1684-1626 cm⁻¹.

14 15 16 **4. Conclusions**

17 A zirconia-supported Pt catalyst was shown to exhibit an unusual band around 1660 cm⁻¹
18 following CO adsorption that could be confidently assigned to a Pt₂-CO bridging carbonyl
19 interacting head-on with a surface hydroxyl group of the support. This adduct was yet unstable in
20 the present conditions and was converted into linear and bridged carbonyl only bound to Pt after

1 a short time. These sites may be of strong catalytic importance in view of the nature of the
2 sorption ensemble (involving atoms at the metal – support interface), but are yet very difficult to
3 investigate because of the many adsorbates (water, carbonates and hydrogenocarbonates) that
4 give rise to bands in the same region.

5

6

7 **Corresponding Author**

8 * e-mail: fcm@ircelyon.univ-lyon1.fr

9 **Author Contributions**

10 The manuscript was written through contributions of all authors. All authors have given approval
11 to the final version of the manuscript.

12 **Funding Sources**

13 None to be acknowledged.

14 **Notes**

15 The authors declare no competing financial interest.

16

17 **ABBREVIATIONS**

18 DRIFTS: Diffuse Reflectance Fourier Transform Infra red Spectroscopy.

19 **REFERENCES**

-
- ¹ "Identification of active sites in CO oxidation and water-gas shift over supported Pt catalysts" K. Ding, A. Gulec, A.M. Johnson, N.M. Schweitzer, D. Stucky, L.D. Marks, P.C. Stair, *Science* 350 (2015) 189-192.
- ² "Catalyst Architecture for Stable Single Atom Dispersion Enables Site-Specific Spectroscopic and Reactivity Measurements of CO Adsorbed to Pt Atoms, Oxidized Pt Clusters, and Metallic Pt Clusters on TiO₂"; L. DeRita, S. Dai, K. Lopez-Zepeda, N. Pham, G.W. Graham, X. Pan, P. Christopher J. *Am. Chem. Soc.* 139 (2017) 14150-14165.
- ³ "Isolated Metal Active Site Concentration and Stability Control Catalytic CO₂ Reduction Selectivity"; J.C. Matsubu, V.N. Yang, P. Christopher, *J. Am. Chem. Soc.* 137 (2015) 3076-3084.
- ⁴ "The influence of surface-defects on the IR-spectra of adsorbed species"; P. Hollins, *Surf. Sci. Rep.* 16 (1992) 51-94.
- ⁵ "Pd oxidation under UHV in a model Pd/ceria-zirconia catalyst"; M. Y. Smirnov, G. W. Graham, *Catal. Lett.* 72 (2001) 39-44.
- ⁶ "Characterization of the standard platinum silica catalyst EUROPT 5. Chemisorption of carbon-monoxide and of oxygen"; P. B. Wells, *Appl. Catal.* 18 (1985) 259-272.
- ⁷ "Direct evidence by in situ IR CO monitoring of the formation and the surface segregation of a Pt-Sn alloy"; A. Moscu, Y. Schuurman, L. Veyre, C. Thieuleux, F. Meunier, *Chem. Commun.* 50 (2014) 8590-8592.
- ⁸ "Correlation between CO frequency and Pt coordination number. A DRIFT study on supported Pt catalysts"; M.J. Kappers, J.H. van der Maas, *Catal. Letters* 10 (1991) 365-374.
- ⁹ "The statistics of surface atoms and surface sites on metal crystals"; R. van Hardeveld and F. Hartog, *Surf. Sci.*, 1969, 15, 189-230.
- ¹⁰ "Effect of preparation technique on the properties of platinum in NaY zeolite: A study by FTIR spectroscopy of adsorbed CO"; K. Chakarova, K. Hadjiivanov, G. Atanasova, K. Tenchev, *J. Mol. Catal. A : Chem.* 264 (2007) 270-279.
- ¹¹ "FTIR spectroscopic study of CO adsorption on Pt-H-ZSM-5"; K. Chakarova, M. Mihaylov, K. Hadjiivanov, *Micropor. Mesopor. Mater.* 81 (2005) 305-312.
- ¹² "Polycarbonyl species in Pt/H-ZSM-5: FTIR spectroscopic study of (CO)-C-12-(CO)-C-13 co-adsorption"; K. Chakarova, M. Mihaylov, K. Hadjiivanov, *Catal. Commun.* 6 (2005) 466-471.
- ¹³ "Thermally stable single-atom platinum-on-ceria catalysts via atom trapping"; J. Jones, H. Xiong, A.T. DeLaRiva, E.J. Peterson, H. Pham, S.R. Challa, G. Qi, S. Oh, M.H. Wiebenga, X.I.P. Hernandez, Y. Wang, A.K. Datye, *Science* 353 (2016) 150-154.
- ¹⁴ "Water-Mediated Mars-Van Krevelen Mechanism for CO Oxidation on Ceria-Supported Single-Atom Pt-1 Catalyst"; C. Wang, X.-K. Gu, H. Yan, Y. Lin, J. Li, D. Liu, W.-X. Li, J. Lu, *ACS Catalysis* 7 (2017) 887-891.
- ¹⁵ "The adsorption of CO on Pt(111) studied by infrared reflection-absorption spectroscopy"; B. E. Hayden, A. M. Bradshaw, *Surf. Sci.* 125, (1983) 787-802.
- ¹⁶ "Probing boundary sites on a Pt/Al₂O₃ model catalyst by CO₂ hydrogenation and in situ ATR-IR spectroscopy of catalytic solid-liquid interfaces"; D. Ferri, T. Burgi, A. Baiker, *Phys. Chem. Chem. Phys.* 4 (2002) 2667-2672.

-
- ¹⁷ “Interaction of CO with Pt supported on ZrO₂(100) – Evidence for CO adsorbed at the Pt-ZrO₂ interface”; P.A. Dilara, J.M. Vohs, *J. Phys. Chem.* 99 (1995) 17259-17264.
- ¹⁸ “Carbonylmetalate-induced phosphorus migration and Ph₂PCH₂PPh₂-(DPPM)-assisted synthesis of bimetallic complexes and clusters of Pd and Pt with Mo, W, Mn, and Co”; P. Braunstein, C. de Méric de Bellefon, B. Oswald, *Inorg. Chem.* 32 (1993) 1649-1655.
- ¹⁹ “Adduct formation and carbonyl rearrangement of polynuclear carbonyls in presence of group III halides”; J.S. Kristoff, D.F. Shriver, *Inorg. Chem.* 13 (1974) 499-506.
- ²⁰ “Infrared spectrometric studies of the surface basicity of metal oxides and zeolites using adsorbed probe molecules”; J.C. Lavalley, *Catal. Today* 27 (1996) 377-401.
- ²¹ K. Nakamoto, “Infrared and Raman Spectra of Inorganic and Coordination Compounds, Part B: Applications in Coordination, Organometallic, and Bioinorganic Chemistry. Sixth Edition”, Wiley Ed., 2009.
- ²² “Infrared spectroscopic identification of species arising from reactive adsorption of carbon oxides on metal-oxide surfaces”; G. Busca, V. Lorenzelli, *Mater. Chem.* 7 (1982) 89-126.
- ²³ “Infrared study of CO₂ adsorption on hematite”; G. Busca, V. Lorenzelli, *Mater. Chem.* 5 (1980) 213-224.
- ²⁴ “Kinetic Studies of the Pt Carbonate-Mediated, Room-Temperature Oxidation of Carbon Monoxide by Oxygen over Pt/Al₂O₃ Using Combined, Time-Resolved XAFS, DRIFTS, and Mass Spectrometry”; M.A. Newton, D. Ferri, G. Smolentsev, V. Marchionni, M. Nachttegaal, *J. Am. Chem. Soc.*, 138 (2016) 13930–13940.
- ²⁵ “IR study of polycrystalline ceria properties in oxidised and reduced states”; C. Binet, M. Daturi, J.-C. Lavalley, *Catal. Today* 50 (1999) 207-225.
- ²⁶ “Participation of surface bicarbonate, formate and methoxy species in the carbon dioxide methanation catalyzed by ZrO₂-supported Ni”; A. Solis-Garcia, J.F. Louvier-Hernandez, A. Almendarez-Camarillo, J.C. Fierro-Gonzalez, *Appl. Catal. B : Env.* 218 (2017) 611-620.
- ²⁷ “An investigation of possible mechanisms of the water-gas shift reaction over a ZrO₂-supported Pt catalyst”; D. Tibiletti, F.C. Meunier, A. Goguet, D. Reid, R. Burch, M. Boaro, M. Vicario, A. Trovarelli, *J. Catal.* 244 (2006) 183-191.
- ²⁸ “An in-situ DRIFTS study of the mechanism of the CO₂ reforming of CH₄ over a Pt/ZrO₂ catalyst”; A.M. O’Connor, F.C. Meunier, J.R.H. Ross, *Stud. Surf. Sci. Catal.* 119 (1998) 819-824.
- ²⁹ “Selective Aerobic Oxidation of 5-HMF into 2,5-Furandicarboxylic Acid with Pt Catalysts Supported on TiO₂- and ZrO₂-Based Supports”; H.Ait Rass, N. Essayem, M. Besson, *ChemSusChem*, 8 (2015) 1206-1217.
- ³⁰ “”; K. Koichumanova, A.K.K. Vikla, R. Cortese, F. Ferrante, K. Seshan, D. Duca, L. Lefferts, *Appl. Catal. B : Env.* 232 (2018) 454-463.
- ³¹ “Interface effect of mixed phase Pt/ZrO₂ catalysts for HCHO oxidation at ambient temperature”; X.Q. Yang, X.L. Yu, M.Y. Lin, M.F. Ge, Y. Zhao, F.Y. Wang, *J. Mater. Chem. A*, 5 (2017) 13799-13806.
- ³² “Nanocrystalline ZrO₂ and Pt-doped ZrO₂ catalysts for low-temperature CO oxidation”; A. Singhania, S.M. Gupta, *Beilstein J. Nanotechnol.* 8 (2017) 264-271.

-
- ³³ “Electrochemical oxidation of ethanol on Pt-ZrO₂/C catalyst”; Y.X. Bai, J.J. Wu, J.Y. Xi, J.S. Wang, W.T. Zhu, L.Q. Chen, X.P. Qiu, *Electrochem. Commun.* 7 (2005) 1087-1090.
- ³⁴ “Electrocatalytic activity of Pt-ZrO₂ supported on different carbon materials for methanol oxidation in H₂SO₄ solution”; R.S. Amin, A.E. Fetohi, R.M.A Hameed, K.M. Khatib, *Int. J. Hydrog. Energy* 41 (2016) 1846-1858.
- ³⁵ “Evolution of the catalytic activity in Pt sulfated zirconia catalysts: Structure, composition, and catalytic properties of the catalyst precursor and the calcined catalyst”; J.M. Manoli, C. Potvin, M. Muhler, U. Wild, G. Resofszki, T. Buchholz, Z. Paal, *J. Catal.*, 178 (1998) 338-351.
- ³⁶ “Hydroisomerisation of n-heptane over Pt/sulfated zirconia catalyst at atmospheric pressure”; F.F. Oloye, R. Aliyev, J.A. Anderson, *Fuel* 222 (2018) 569-573.
- ³⁷ “A modified commercial DRIFTS cell for kinetically relevant operando studies of heterogeneous catalytic reactions”; F.C Meunier, A. Goguet, S. Shekhtman, D. Rooney, H. Daly, *Appl. Catal. A: Gen.* 340 (2008) 196-202.
- ³⁸ “Effective bulk and surface temperatures of the catalyst bed of FT-IR cells used for in situ and operando studies”; H. Li, M. Rivallan, F. Thibault-Starzyk, A. Travert, F.C Meunier, *Phys. Chem. Chem. Phys.* 15 (2013) 7321-7327.
- ³⁹ “Quantitative analysis of adsorbate concentrations by diffuse reflectance FT-IR”; J. Sirita, S. Phanichphant, F.C. Meunier, *Anal. Chem.* 79 (2007) 3912-3918.
- ⁴⁰ “An infrared study of sulfated zirconia”; M. Bensitel, O. Saur, J.-C. Lavalley, *Mater. Chem. Phys.* 19 (1988) 147-156.
- ⁴¹ “A thermogravimetric and FT-IR study of the reduction by H₂ of sulfated Pt/Ce_xZr_{1-x}O₂ solids”; P. Bazin, O. Saur, F.C. Meunier, M. Daturi, J.C. Lavalley, A.M. LeGovic, V. Harle, G. Blanchard, *Appl. Catal. B : Env.* 90 (2009) 368-379.
- ⁴² “CO Oxidation Kinetics over Au/TiO₂ and Au/Al₂O₃ Catalysts: Evidence for a Common Water-Assisted Mechanism”; J. Saavedra, C.J. Pursell, B.D. Chandler, *J. Am. Chem. Soc.* 140 (2018) 3712-3723.